



Harmful Gas Molecule Detection Using Lithium Doped Graphene: Theoretical Analysis of Adsorption and Gas-Sensing Properties

Salah Abdul Mahdi Khudair 

Directorate General of Education in Babylon Governorate, Ministry of Education, Babylon 51001, Iraq

Corresponding Author Email: salahalmahdi30@gmail.com

Copyright: ©2025 The author. This article is published by IIETA and is licensed under the CC BY 4.0 license (<http://creativecommons.org/licenses/by/4.0/>).

<https://doi.org/10.18280/acsm.490612>

Received: 2 November 2025

Revised: 2 December 2025

Accepted: 9 December 2025

Available online: 31 December 2025

Keywords:

adsorption, density of states, density functional theory, energy gap, gas sensor, harmful gas molecule, Li-doped graphene

ABSTRACT

In the present paper, the energetic, structural, geometric, and electronic characteristics of graphene (Gr) were examined with the use of first-principles density functional theory (DFT) methods in relation to adsorption of CO, CO₂, NH₃, SO₂, and N₂ molecules and to lithium (Li) contamination. They substituted a single carbon (C) atom with a Li atom, creating an energy gap (E_g) of 0.08 eV. We calculated a range of E_g values by using different doping and adsorption techniques with Li. The highest value we obtained was 0.80 eV. The results indicate that CO, NH₃, and SO₂ molecules undergo physical adsorption onto the surface of Li-doped graphene (Li-Gr), with adsorption energy (E_{ad}) values of -0.31, 0.56, and 0.93 eV, respectively. On the other hand, CO₂ and N₂ molecules are chemically bonded to the surface of Li-Gr, with E_{ad} values of -2.44 and -1.08 eV, respectively. In contrast, CO₂ and N₂ molecules are chemisorbed on the Li-Gr surface, with E_{ad} values of -2.44 and -1.08 eV, respectively. The results of our calculations indicate that Li-Gr may be a suitable sensor for CO, NH₃, and SO₂ molecules. Using the DFT approach, we determined the optimal and stable electronic configurations of Li-Gr.

1. INTRODUCTION

Greenhouse and toxic gases such as CO₂, NO₂, CO, SO₂, and NH₃ are major pollutants emitted from industrial processes, contributing to global climate change and environmental challenges. Therefore, due to the ecological issues and climate change humanity is currently facing, there has been a growing need for carbon (C) nanostructures capable of enabling rapid green operations [1]. Graphene (Gr), a material with a highly compact two-dimensional (2D) lattice structure composed of C atoms, presents a viable answer [2]. Chemically modifying Gr is a realistic method to improve its chemical and physical characteristics. Metal doping has proven effective in modifying its electronic structure and strengthening gas binding. Among these metals, lithium (Li) stands out for its ability to increase electron density around adjacent C atoms, creating active adsorption sites. More precisely, modifying the covalent bonds in Gr can significantly alter its electrical configuration. This can be accomplished by either chemically modifying the Gr structure [3-10] or by integrating heteroatoms into the Gr framework [11-16].

The use of intelligent sensors in our daily lives is a phenomenon that has been steadily increasing over the last two decades [17]. Nowadays, sensors can be found in virtually all areas of life, including industry, homes, and the environment, with the goal of improving the overall quality of life [18-21]. Electrodes are also important components of sensor systems, facilitating the analysis and transmission of sensed data to the monitoring unit.

It has been observed that ongoing research efforts have

focused on developing electrode materials to improve their electrical, thermal, and mechanical properties. Commonly used electrode materials include aluminum, silver, and gold [22-24]. Gr, which is a material with unique electrical and crystallographic characteristics, is always in demand. This material consists of a monolayer of C atoms and has a structure resembling a 2D honeycomb crystal lattice [25].

Gas sensing technology has also made significant advances, exploiting nanomaterials, driven by rapid advances in materials science. Gr has advanced significantly in gas sensing as a result of its unique geometrical structure, large specific surface area, and outstanding electrical characteristics [26]. Gr has also excelled in one area, the development of gas sensors with outstanding performance [27]. Nonetheless, Gr reacts poorly with most of the gas molecules.

It is, therefore, imperative to employ the right methods and make Gr more attentive and efficient. Theoretical and experimental studies have suggested that one viable method to improve the gas-sensing properties of 2D nano-materials is to dope them [28].

The electrical characteristics of Gr are significantly enhanced by doping. Further investigation has shown that the existence of doped atoms can alter both the arrangement of energy levels and the process of electron transfer in Gr, thereby significantly enhancing its possible uses [29]. Out of all the different metal elements, it is important to mention that Li has been widely used for introducing impurities into Gr. Researchers have extensively studied the potential of Li-doped graphene (Li-Gr) as an adsorbent for gaseous molecules in several academic papers [30]. An example of this would be the

use of Li atoms in the process of doping Gr for a variety of applications. By releasing electrons through nearby C atoms, doping Gr with Li causes an increase in the electron density surrounding the doped atom. This is because the doped atom releases electrons. By virtue of this rise in charge, the Li atom is transformed into an essential location that is favorable to adsorption of gas molecules onto Gr [31, 32]. Hence, a model of Li-Gr is presented in this study. A variety of molecules, including CO, CO₂, NH₃, SO₂, and N₂, were studied for their adsorption capabilities on surface of Li-Gr. Through computer analysis, the following parameters were determined: geometric structures, adsorption distance, bond length, adsorption energy (E_{ad}), band energy gap (E_g), Fermi energy (E_F), and density of states (DOS). We also compared computational outcomes of adsorbed gases on the Li-Gr surface. These results helped to clarify the processes of contact and adsorption. Insights into gas molecule detection will be greatly enhanced by our investigation. Pure Gr's low E_{ad} limit its reactivity to many harmful gases, despite the material's potential gas detection uses [33]. The modification of the electronic structure and the enhancement of E_{ad} are two of the ways that doping Gr with a variety of elements has been investigated as a potential method for improving its gas-sensing capabilities [34]. However, there is a need for additional research that is more extensive in nature about the gas-sensing capabilities of Li-Gr. Using first-principles density functional theory (DFT) computations, the primary objective of the present investigation is to analyze adsorption of hazardous gas molecules on Li-Gr. These gas molecules include CO, CO₂, N₂, and SO₂. To investigate E_{ad} as well as changes in electronic structure that occur during gas adsorption for the purpose of gaining an understanding of gas sensing mechanisms. In order to conduct a comprehensive analysis of gas-sensing capabilities of Li-Gr with respect to a variety of gases. The purpose of this project is to guide the practical development of high-performance dangerous gas sensors based on Li-Gr by providing theoretical guidance.

The proposed research aims to achieve these goals to address the current research gap and demonstrate that Li-Gr is a highly promising material in the detection of hazardous gas molecules. The DFT simulations will provide in-depth atomic insight into the gas-sensing characteristics that can guide the rational design of progressively novel gas sensors based on Gr. The findings will contribute to the advancement of gas sensors to monitor the environment, provide security, and other spheres.

2. MATERIALS AND METHODS

2.1 Computational details

Gr sheet model has been created with the use of the Nanotube Modeler software. The shape and energy estimates for Li-Gr were thoroughly optimized with the use of DFT, both with and without the presence of gas molecules. DFT is a widely utilized approach for analyzing the electronic structures of molecules.

It is characterized by its high accuracy and relatively low processing cost, hence it is a favorite in determining the features of the ground state. The calculated values were made through the Gaussian 09 program package and displayed through the GaussView 5.0 [35]. In this sense, we can look at our optimized structures.

The Gauss Sum software was used to obtain the findings of the DOS. The analysis of electron exchange and correlation interactions was done through generalized gradient approximation (GGA) by the Perdew-Burke-Ernzerhof (PBE) functional approach [36], with a 6-31G basis set. This has been applied effectively on Gr-based materials onto which small gas molecules are adsorbed [37-39].

The Li-Gr model was designed, and a core of C atoms was substituted with Li atoms to give the system of 42 C atoms in Li-Gr. This structure has a dopant concentration of 2.4% in the Li-Gr structure.

The gas molecules' E_{ad} on Li-Gr (E_{ad (gas+ Li-Gr)}) can be calculated using the following formula [40-42]:

$$E_{ad(gas+Li-Gr)} = E_{(gas+Li-Gr)} - [E_{Li-Gr} + E_{gas}] \quad (1)$$

In this equation, E_(gas+Li-Gr) denotes total energy of the relaxed molecule on Li-Gr, E_{Li-Gr} denotes energy of isolated Li-Gr, and E_{gas} denotes energy of the isolated gas molecule.

The interaction mechanism is explained by the fact that the highest occupied molecular orbital (E_{HOMO}) and the lowest unoccupied molecular orbital (E_{LUMO}) in free Li-Gr and gas molecules adsorbed on Li-Gr have differential energy levels. The HOMO is identified as an electron donor as a result of its presence of a large number of electrons, whereas the electron-deficient electron is the LUMO, and it shows the electron-accepting property [43].

2.2 Computational models

The structure of graphite had been optimized to give the Gr model. Gr has a very stable and symmetrical atomic structure, which means the presence of a hexagonal monolayer. The chemical equation of the substance is C, and every C atom covalently bonds to 3 other C atoms in a honeycomb structure. Figure 1 is a Gr model that was prepared using a 3 × 3 supercell. The lengths of the C-C bonds are 1.42 Å [44], which is a proven fact as seen in the literature [45].

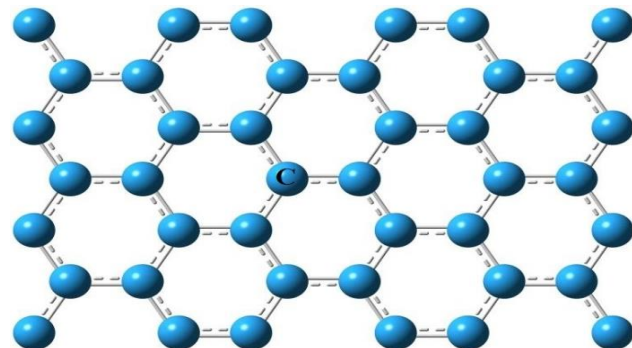


Figure 1. Model of (3 × 3) Gr in the present study

3. RESULTS AND DISCUSSION

Gr surface was also doped with Li atoms, which are donors of electrons to enhance the level of binding [46]. This change significantly alters the geometry of the doped Gr, as shown in Figure 2. The reduction in the C-C bond length indicates that this bond is stronger than Li-C bond, since the change in the length indicates this. Pristine Gr is estimated to have the length of C-C bond of 1.42 Å [40]. The Li-C bond length is 0.25 Å

in comparison with the C–C bond length of pristine Gr. Moreover, there is a low perturbation of C–C bond lengths, which are slightly offset from the dopant. Such findings are corroborated by the previous literature [46]. Following intensive relaxation, Li-Gr preserves the planar shape of Gr, although such alterations [15].

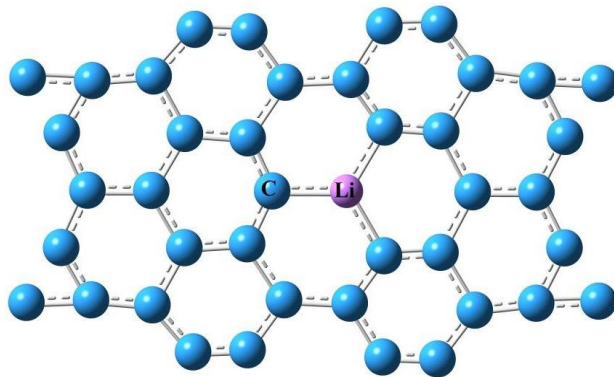


Figure 2. The optimized structure of Li-Gr

Table 1 shows Li contamination effect on the electronic behavior of Gr. The addition of Li into the Gr structure affects its electronic properties. It should also be mentioned that the Li-Gr E_g value lies around 0.083 eV. This means that Li doping enhances the conductivity of Gr, making it very suitable to use in applications where conductive or semi-conductive materials are required. E_g [47] is calculated with the use of the following formula:

$$E_g = E_{LUMO} - E_{HOMO} \quad (2)$$

As evident from Table 1, the E_F is -4.449 eV, calculated with the use of the formula [43].

$$E_F = (E_{HOMO} + E_{LUMO})/2 \quad (3)$$

Table 1. The electronic characteristics of Li-Gr

Property (eV)	Li-Gr
E_g	0.083
E_{HOMO}	-4.490
E_{LUMO}	-4.407
E_F	-4.449

Li is a popular phenomenon that has been observed in this work as well. The shallow donor impurities generate energy levels in the region where conduction band edge is, and the shallow acceptor impurities generate energy levels in the region close to the valence band edge [48].

The increasing Li concentration causes the corresponding DOS of the impurities to increase, and this, in effect, forms a continuous spectrum of energy levels just as the bands do, effectively reducing the E_g . In essence, Li acts as an n-type dopant, and it adds electron-doping properties, which lead to the Dirac point shifting below the E_F . The electron doping pushes most states to be below the E_F , which causes a decrease in the E_g .

According to the results, Li doping is one of the effective methods to alter electronic characteristics of the Gr in terms of the bandgap decrease and the increase in the conductivity [49]. The Li atoms also add shallow donor levels that allow the occupancy of electrons and cause a Dirac point shift. This

change identifies processes by which doping affects electronic band structure.

The valence band and conduction band each contain a number of primary peaks. A representation of the DOS can be found in Figure 3, where it is demonstrated that the maximum number of degenerate states that can be found in both bands for Li-Gr is four. When it comes to certain energy levels, it is evident that states which are available for occupancy at high levels of DOS [50] are those that are available. On the other hand, it is mathematically impossible to inhabit any state that has a zero-DOS energy level [51].

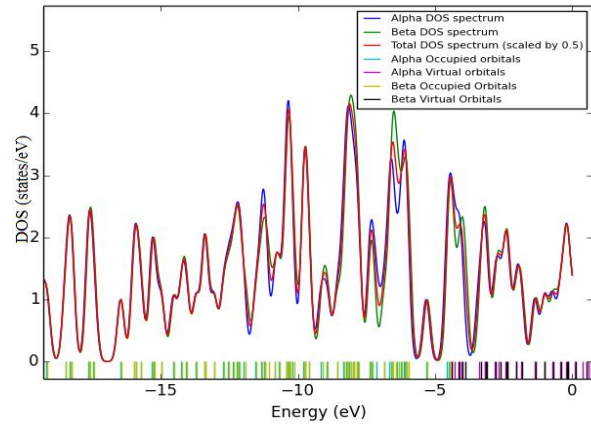


Figure 3. Plot of DOS for Li-Gr, Red line Alpha DOS spectrum, and blue line Beta DOS spectrum

The Li-Gr is being investigated to enhance its interaction with gaseous molecules. Since Li possesses one additional valence electron when compared to C, such doping results in an n-type semi-conductor where electrons are the primary carriers, implying that Li acts as a donor.

On the other hand, the gas molecules act as acceptors, which contribute to a substantial transfer of charges [51]. As a result, there is great interaction between the electron-deficient gas molecules and the electron-donating atoms of Li. This is the reason why gas molecules are absorbed on the Li sites instead of interacting with the Gr C [40].

The energetic data of the systems have been computed, which includes E_{ad} , E_g energies, HOMO energies, LUMO energies, and Fermi level energies as in Table 2. We examine adsorption of gases, NH_3 , SO_2 , CO , CO_2 , and N_2 , on Li-Gr around the dopant position. We then discuss their effects on the electrical and structural characteristics of Li-Gr. Figure 4(a) shows the optimized adsorption structure of CO on Li-Gr.

Additionally, we observe that the adsorption distance of Li-C between the adsorbed CO molecule on a Li-Gr surface is 1.73 Å, which generally decreases with the increase of electrons in the elements [52]. Moreover, the angle of Li-C-O is 96°. As observed from Table 2, the E_{ad} for Li-Gr is -0.309 eV; this result is consistent with previous findings [53], indicating physisorption [53- 55]. The binding strength of CO to Li-Gr is moderate based on this E_{ad} value. Therefore, Li-Gr can effectively detect CO, given the ease with which the adsorption-desorption equilibrium of CO on Li-Gr can be established. Figure 4(b) illustrates the most stable configuration of adsorbed CO_2 on Li-Gr. It has been observed that the adsorption distance of Li-C between adsorbed CO_2 molecules on a Li-Gr surface is 1.73 Å, which generally decreases with an increase in the electron count of the elements. Meanwhile, the angle between the adsorption

distance of Li-C and plane of Li-Gr is 96° , similar to the adsorption of CO on Li-Gr. The calculated E_{ad} was -2.435 eV. We note that our result is fairly similar to previous reports [56], indicating strong chemisorption [57], significantly surpassing the adsorption intensity of CO on Li-Gr. However, CO_2 on Li-Gr could catalyze or activate this adsorbate as a result of the robust interaction, implying the potential of Li-Gr as a catalyst. The NH_3 molecule is adsorbed onto Li-Gr via Li-atoms, as illustrated in Figure 4(c). We observe that the adsorption distance of Li-N between adsorbed NH_3 molecules on a Li-Gr surface measures 1.69 \AA , which generally decreases with an increase in the electron count of the elements. Additionally, the angle between adsorption distance of Li-N and plane of Li-Gr is 85° . The overall results of adsorbed NH_3 on Li-Gr have been summarized in Table 2. E_{ad} indicates that the tying strength of NH_3 with Li-Gr is 0.560 eV, which is consistent with the other results [58]. Hence, Li-Gr

can serve as a means to detect NH_3 .

The SO_2 molecule is adsorbed onto Li-Gr via Li atoms, as can be seen from Figure 4(d). Adsorption distance of Li-S between adsorbed SO_2 molecules on a Li-Gr surface is 1.73 \AA , and we note that our results are fairly similar to previous reports [59], and the angle between the adsorption distance of Li-S and the plane of Li-Gr is 88° . According to the results in Table 2, the E_{ad} of SO_2 on Li-Gr is 0.927 eV, this result is well in accordance with the earlier findings [60], indicating a strong physisorption. This suggests that Li-Gr is sensitive to SO_2 gas. The N_2 molecule is adsorbed onto Li-Gr via Li atoms, as can be seen in Figure 4(e). The adsorption distances of Li- N_1 and Li- N_2 between adsorbed N_2 molecules on a Li-Gr surface are 1.78 \AA and 2.02 \AA , respectively, and the Li- N_1 - N_2 angle is 84° . The sensitivity of Li-Gr has been enhanced, rendering it a very efficient sensor for the detection of N_2 molecules.

Table 2. The structural and electronic characteristics of various gases that are adsorbed on Li-Gr

Device	Gas	E_{ad} (eV)	E_g (eV)	E_{HOMO} (eV)	E_{LUMO} (eV)	E_F (eV)
Li-Gr	CO	-0.309	0.147	-4.785	-4.638	-4.712
	CO_2	-2.435	0.804	-5.694	-4.890	-5.292
	NH_3	0.560	0.056	-4.288	-4.232	-4.260
	SO_2	0.927	0.234	-4.856	-4.622	-4.739
	N_2	-1.083	0.088	-4.172	-4.084	-4.128

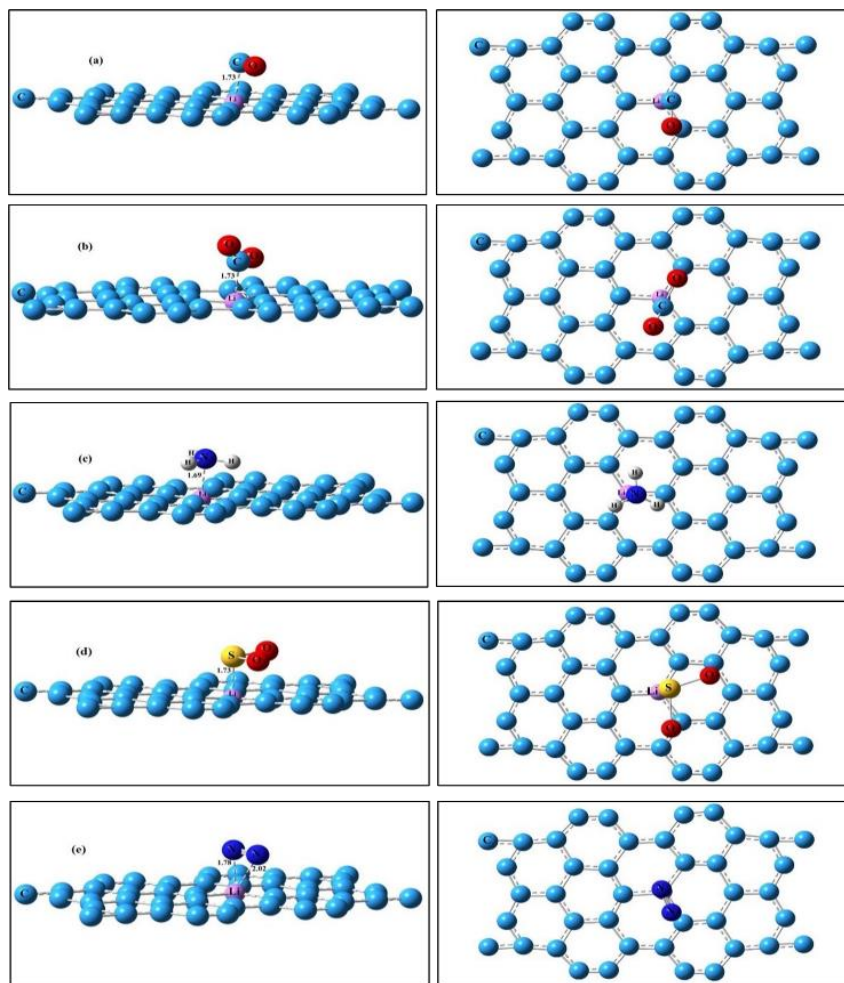


Figure 4. Top and side views of optimized structures and key bond length of the gas molecules (a) CO , (b) CO_2 , (c) NH_3 , (d) SO_2 , and (e) N_2 adsorbed on Li-Gr

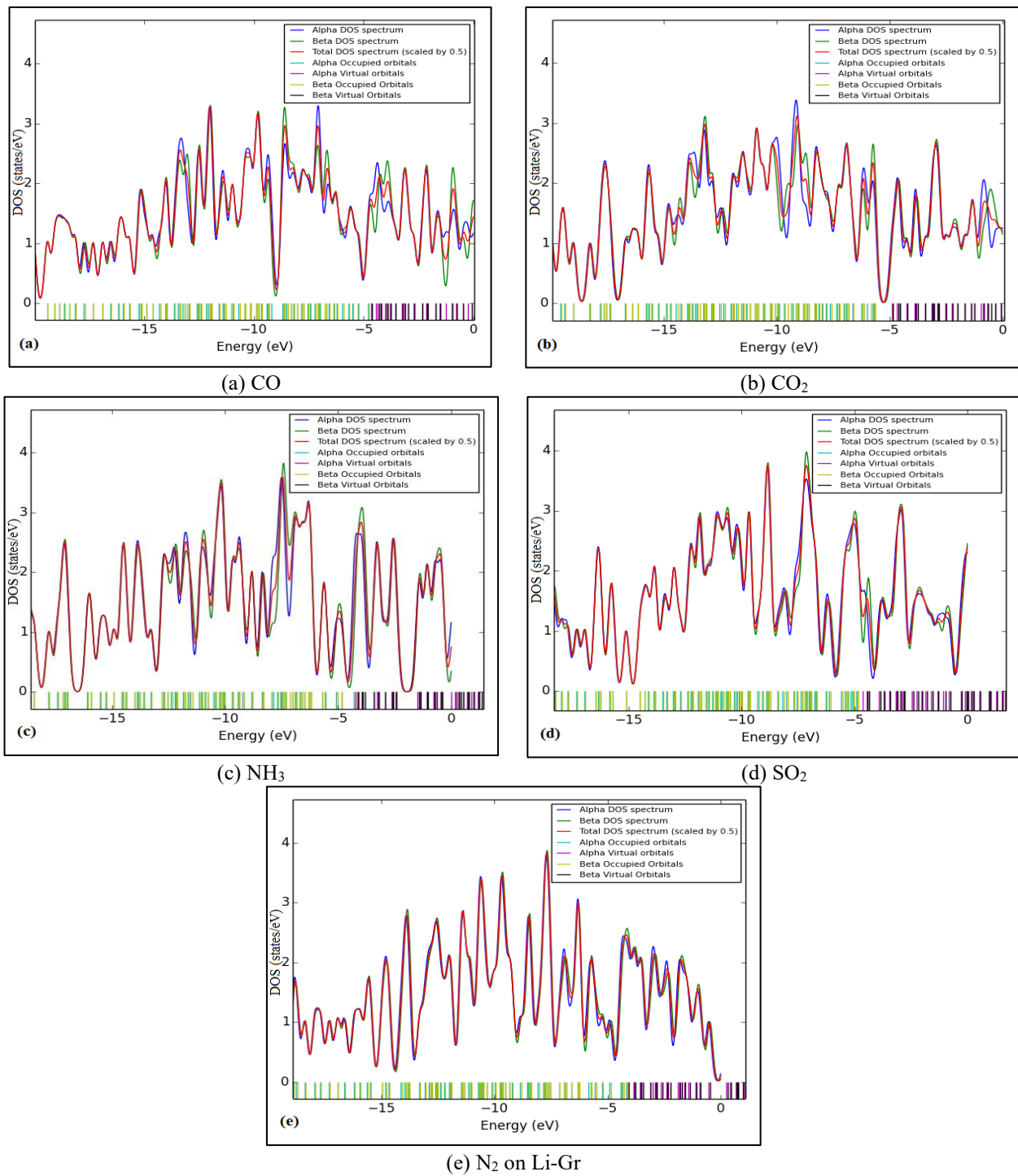


Figure 5. DOS for the adsorbate

The data presented in Table 2 shows that Li-Gr is a considerably electrically sensitive material to the N_2 presence in the material surface as depicted by the E_{ad} value of -1.083 eV. It should be noted that our results are consistent with previous research [61] to a certain degree. This implies the medium chemisorption interaction. Hence, Li-Gr shows a good electronic response to the N_2 molecules, which implies that such a system can catalyze or activate the aforementioned adsorbate because of the high contact. This implies that Li-Gr can be utilized as a catalyst.

The electronic interaction, as indicated in Table 2, between the adsorbate and the Li dopant, as an electron-donating active site, determines the adsorption behavior of gas molecules on Li-Gr. Surface polarization with no significant charge transfer

controls the weak adsorption of CO (-0.309 eV), which is primarily physisorption and also shows good reversibility in sensing.

NH_3 has a moderate binding strength (0.560 eV) because the nitrogen lone pair and Li are coordinated, which guarantees a balanced sensitivity response and stability response. CO_2 (-2.435 eV) has a very strong interaction, which is attributed to the fact that the charge transfer to its antibonding orbitals is very high, resulting in chemisorption and the activation of the molecules.

The physisorption of SO_2 (0.927 eV) is high due to its high polarity and electrostatic interactions, which gives a high sensing sensitivity. N_2 , on the other hand, exhibits moderate chemisorption (-1.083 eV) because of a partial charge transfer

between the Li-induced electronic states around the Fermi level, implying an enhanced electrical reaction and possible catalytic activity.

Overall, Li doping modifies the electronic structure of Gr and leads to distinct adsorption strengths following the trend $\text{CO} < \text{NH}_3 < \text{SO}_2 < \text{N}_2 < \text{CO}_2$, in good agreement with energetic data in Table 2.

Results in Table 2 show that E_g after adsorption of CO, CO_2 , SO_2 , and N_2 gases on Li-Gr is larger than the E_g before adsorption. This indicates that E_g increases with the adsorption on Li-Gr. Li atoms add electrons to Gr, altering its electronic properties. Gas molecules' adsorption can lead to withdrawal or re-distribution of some of these electrons, thereby increasing the E_g between valence band and conduction band. In contrast, the E_g after adsorption of NH_3 gas on Li-Gr is smaller than the E_g before adsorption.

NH_3 is also an electron donor, and as the NH_3 molecules adsorb onto the Li-Gr surface, they donate electrons to the Gr, introducing additional electrons to the system. This causes the energy levels that are nearer to the conduction band to fill and thus lowering the E_g . Computed E_F of Li-Gr at the end of the adsorption of CO, CO_2 , and SO_2 is greater when compared to the one before adsorption, but the computed E_F of Li-Gr at the end of the adsorption of NH_3 and N_2 is less than the one before adsorption.

The Li-doped surface will be able to present active adsorption sites, which will increase the number of interactions between the gas molecules and Gr. These interactions may cause a change in the electronic state of Gr, and consequently increase or decrease the E_F . Calculated results have shown that E_{HOMO} of the molecule is (-5.694 eV),

implying that it has a tendency to donate electrons. Conversely, the E_{LUMO} of the molecule is (-4.084 eV), with implications of a tendency to accept electrons.

For the purpose of further exploring electronic characteristics of studied structures, DOS plots have been calculated of the adsorbed Li-Gr respectively, Figures 5(a)-(e) depict that the DOS of Li-Gr with adsorption of gas molecules CO, CO_2 , NH_3 , SO_2 and N_2 is not the same as the one of the DOS before the adsorption. The heights of the peaks become smaller, meaning that the number of DOS peaks in conduction band as well as valence band becomes smaller.

Adsorption of gases can lead to distortions in the Gr structure or surface reactions that result in changes in the energy distribution of electronic states. This can sometimes lead to a reduction in peak height or a decrease in DOS peaks.

The role of frontier molecular orbitals (FMOs), specifically LUMO and HOMO, is well-established in chemical reactions involving reactant molecules. For the analysis of the Li-Gr, understanding the FMOs becomes essential. In our study, we have summarized HOMO and LUMO energy levels for gas molecules like CO, CO_2 , NH_3 , SO_2 , and N_2 adsorbed on Li-Gr in Table 2. Figures 6 and 7 show the analyzed structures of 3-D HOMO and LUMO distributions. The electron cloud in occupied and virtual orbitals is clearly seen in HOMO-LUMO. Structures have HOMO electrons in green and LUMO electrons in red. DOS spectra for Li-Gr structures show low occupied orbital charge density and high virtual orbital charge density. This describes charge localization in virtual orbitals versus occupied orbitals. The FMOs of these gas molecules are concentrated in the Li-Gr structures' center and edges.

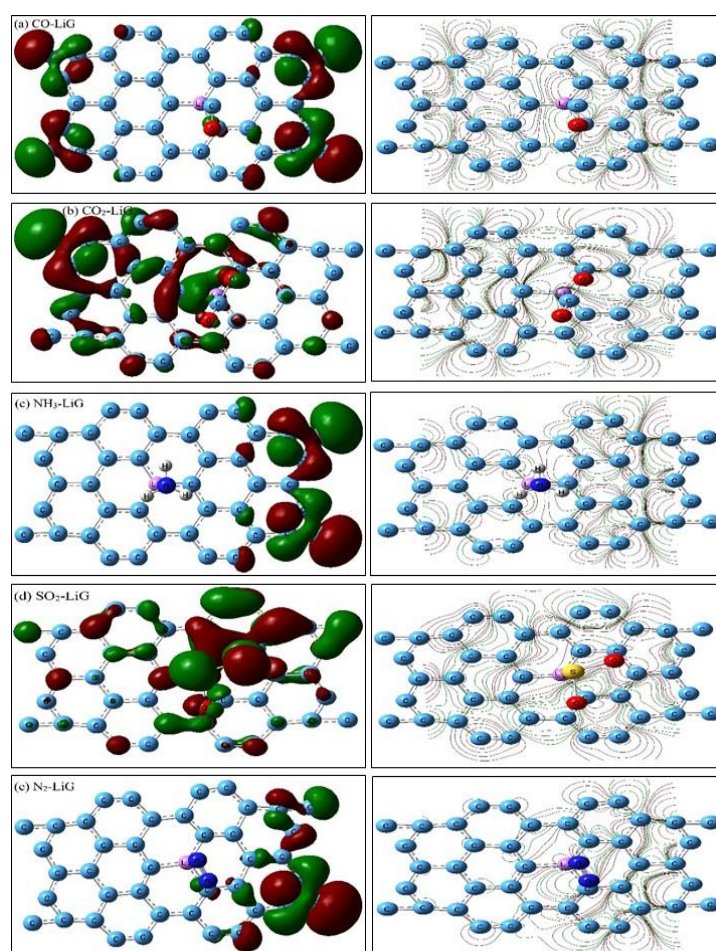


Figure 6. HOMO distribution (right: 2-D counter; left: 3-D) in Li-Gr structures

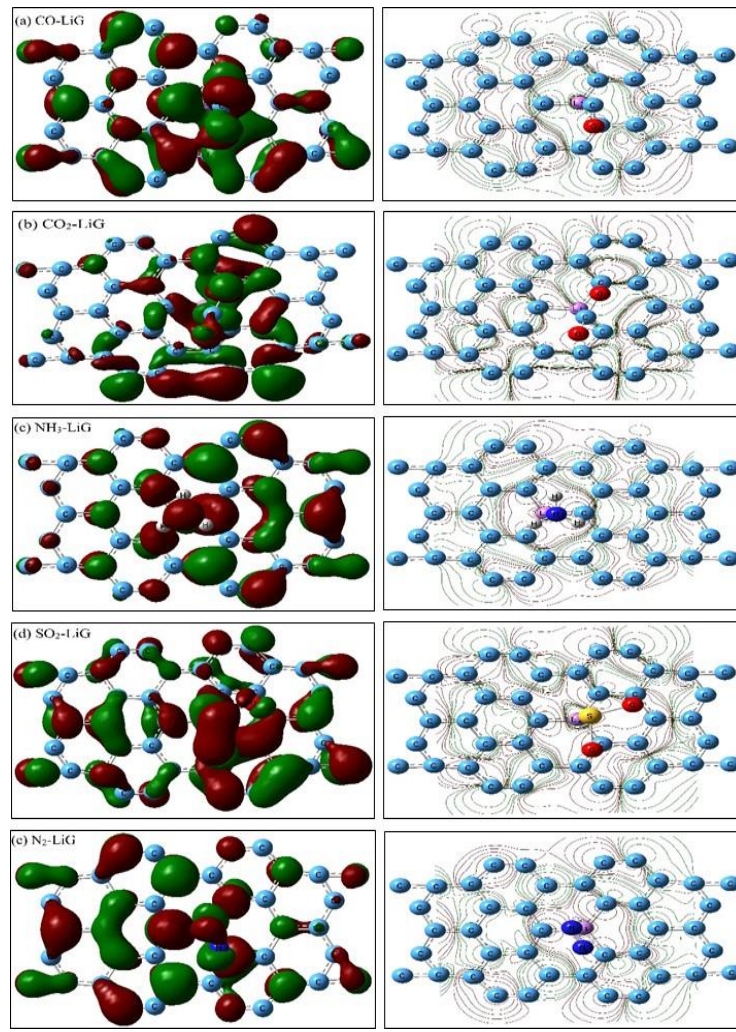


Figure 7. LUMO distribution (right: 2-D counter; left: 3D) in Li-Gr structures

Our theoretical predictions could be validated experimentally using techniques such as TPD, XPS, or conductivity measurements, providing a pathway to test the adsorption behavior and sensitivity of Li-Gr toward CO, CO₂, NH₃, SO₂, and N₂.

4. CONCLUSIONS

This article studied the interaction between Li-Gr and CO, CO₂, NH₃, SO₂, and N₂ molecules in a systematic way through the use of DFT. On adsorbing these gas molecules, the electronic structure of Li-Gr is observably altered, with shifts in the Fermi level of the material being indicative of n-type behavior. These electrical additions indicate that Li doping amplifies the interaction between Gr and gas molecules, which is pertinent in sensing-related applications.

The calculated E_{ad} shows that the interactions between CO₂ and N₂ and Li-Gr are very strong and have more characteristics that are associated with chemisorption. This high degree of binding would mean a low level of reversibility, and so could be of limited use in sensing applications, but could imply the presence of an application in catalytic or capture-related applications. CO, NH₃, as well as SO₂, on the other hand, are moderated with E_{ad} and adsorption distance, which are indicative of physisorption. The characteristics are mostly related to reversible adsorption, which is a desirable property in gas sensing.

Overall, the present results demonstrate that Li doping significantly alters the electronic characteristics of Gr and modulates its interaction with different gas molecules. While the findings indicate that Li-Gr may be a potential candidate for sensing CO, NH₃, and SO₂, further experimental validation and performance evaluation are required to assess its practical applicability. The insights provided here contribute to a fundamental understanding of gas-Gr interactions and may assist in the rational design of Gr-based sensing materials.

REFERENCES

- [1] Barra, A., Nunes, C., Ruiz-Hitzky, E., Ferreira, P. (2022). Green carbon nanostructures for functional composite materials. *International Journal of Molecular Sciences*, 23(3): 1848. <https://doi.org/10.3390/ijms23031848>
- [2] Taha, H.O., El Mahdy, A.M., Lebda, H.I. (2024). Adsorption of gases on doped graphene quantum dots with (TM = Ni, Pd, and Pt): DFT and TD-DFT investigation. *Physica B: Condensed Matter*, 676: 415667. <https://doi.org/10.1016/j.physb.2024.415667>
- [3] Ijeomah, G., Samsuri, F., Obite, F., Zawawi, M.A.M. (2020). Recent advances in chemical functionalisation of graphene and sensing applications. *International Journal of Biomedical Nanoscience and Nanotechnology*, 4(1-2): 1-48. <https://doi.org/10.1504/IJBN.2020.107177>
- [4] Mishyn, V., Rodrigues, T., Leroux, Y.R., Aspermair, P.,

et al. (2021). Controlled covalent functionalization of a graphene-channel of a field effect transistor as an ideal platform for (bio) sensing applications. *Nanoscale Horizons*, 6(10): 819-829. <https://doi.org/10.1039/D1NH00355K>

[5] Shin, D., Kim, H.R., Hong, B.H. (2021). Gold nanoparticle-mediated non-covalent functionalization of graphene for field-effect transistors. *Nanoscale Advances*, 3(5): 1404-1412. <https://doi.org/10.1039/D0NA00603C>

[6] Văduva, M., Baibarac, M., Cramariuc, O. (2022). Functionalization of graphene derivatives with conducting polymers and their applications in uric acid detection. *Molecules*, 28(1): 135. <https://doi.org/10.3390/molecules28010135>

[7] Jain, V., Kandasubramanian, B. (2020). Functionalized graphene materials for hydrogen storage. *Journal of Materials Science*, 55(5): 1865-1903. <https://doi.org/10.1007/s10853-019-04150-y>

[8] Maio, A., Pibiri, I., Morreale, M., Mantia, F.P.L., Scaffaro, R. (2021). An overview of functionalized graphene nanomaterials for advanced applications. *Nanomaterials*, 11(7): 1717. <https://doi.org/10.3390/nano11071717>

[9] Huang, H., Shi, H., Das, P., Qin, J., et al. (2020). The chemistry and promising applications of graphene and porous graphene materials. *Advanced Functional Materials*, 30(41): 1909035. <https://doi.org/10.1002/adfm.201909035>

[10] Andrade-Guel, M., Cabello-Alvarado, C., Cruz-Delgado, V.J., Bartolo-Perez, P., et al. (2019). Surface modification of graphene nanoplatelets by organic acids and ultrasonic radiation for enhance uremic toxins adsorption. *Materials*, 12(5): 715. <https://doi.org/10.3390/ma12050715>

[11] Yu, W., Sisi, L., Haiyan, Y., Jie, L. (2020). Progress in the functional modification of graphene/graphene oxide: A review. *RSC Advances*, 10(26): 15328-15345. <https://doi.org/10.1039/D0RA01068E>

[12] Clancy, A.J., Au, H., Rubio, N., Coulter, G.O., Shaffer, M.S. (2020). Understanding and controlling the covalent functionalisation of graphene. *Dalton Transactions*, 49(30): 10308-10318. <https://doi.org/10.1039/D0DT01589J>

[13] Abdelazeez, A.A.A., Ben Gouider Trabelsi, A., Alkallas, F.H., AlFaify, S., et al. (2023). Tuning the structural, electronic, and optical properties of monolayer graphene through heteroatom doping: A first-principles study with future light sensing applications. *Photonics*, 10(7): 838. <https://doi.org/10.3390/photonics10070838>

[14] Kasibhatta, K.R.D., Madakannu, I., Prasanthi, I. (2021). Hetero atom doped graphene nanoarchitectonics as electrocatalysts towards the oxygen reduction and evolution reactions in acidic medium. *Journal of Inorganic and Organometallic Polymers and Materials*, 31(5): 1859-1876. <https://doi.org/10.1007/s10904-020-01834-w>

[15] Jappor, H.R., Khudair, S.A.M. (2017). Electronic properties of adsorption of CO, CO₂, NH₃, NO, NO₂ and SO₂ on nitrogen doped graphene for gas sensor applications. *Sensor Letters*, 15(5): 432-439. <https://doi.org/10.1166/sl.2017.3819>

[16] Joucken, F., Henrard, L., Lagoute, J. (2019). Electronic properties of chemically doped graphene. *Physical Review Materials*, 3(11): 110301. <https://doi.org/10.1103/PhysRevMaterials.3.110301>

[17] Nag, A., Mukhopadhyay, S.C., Kosel, J. (2016). Flexible carbon nanotube nanocomposite sensor for multiple physiological parameter monitoring. *Sensors and Actuators A: Physical*, 251: 148-155. <https://doi.org/10.1016/j.sna.2016.10.023>

[18] de Fátima Muniz, R., Muniz, S.M. (2023). Investigation of IoT-Integrated Smart Homes. *Journal of Operational and Strategic Analytics*, 1(1): 42-45. <https://doi.org/10.56578/josa010106>

[19] Nag, A., Mitra, A., Mukhopadhyay, S.C. (2018). Graphene and its sensor-based applications: A review. *Sensors and Actuators A: Physical*, 270: 177-194. <https://doi.org/10.1016/j.sna.2017.12.028>

[20] Trigona, C., Graziani, S., Baglio, S. (2020). Changes in sensors technologies during the last ten years: Evolution or revolution. *IEEE Instrumentation & Measurement Magazine*, 23(6): 18-22. <https://doi.org/10.1109/MIM.2020.9200876>

[21] Mah, P.M., Skalna, I., Pełech-Pilichowski, T., Muzam, J., Munyeshuri, E., Uwakmfon, P.O., Mudoh, P. (2022). Integration of sensors and predictive analysis with machine learning as a modern tool for economic activities and a major step to fight against climate change. *Journal of Green Economy and Low-Carbon Development*, 1(1): 16-33. <https://doi.org/10.56578/jgelcd010103>

[22] Javaid, M., Haleem, A., Rab, S., Singh, R.P., Suman, R. (2021). Sensors for daily life: A review. *Sensors International*, 2: 100121. <https://doi.org/10.1016/j.sintl.2021.100121>

[23] Mourzina, Y.G., Ermolenko, Y.E., Offenhäusser, A. (2021). Synthesizing electrodes into electrochemical sensor systems. *Frontiers in Chemistry*, 9: 641674. <https://doi.org/10.3389/fchem.2021.641674>

[24] Theyagarajan, K., Kim, Y.J. (2023). Recent developments in the design and fabrication of electrochemical biosensors using functional materials and molecules. *Biosensors*, 13(4): 424. <https://doi.org/10.3390/bios13040424>

[25] Kumar, S., Himanshi, Prakash, J., Verma, A., et al. (2023). A review on properties and environmental applications of graphene and its derivative-based composites. *Catalysts*, 13(1): 111. <https://doi.org/10.3390/catal13010111>

[26] Huang, L., Zhai, X., Liu, H., Gu, L., Cui, W., Gu, X. (2024). Transition metal doped 2D SiC (TM = Ag, Pd and Rh) as a potential candidate for NO_x (x = 1, 2) and NH₃ sensing. *Sensors and Actuators A: Physical*, 367: 115062. <https://doi.org/10.1016/j.sna.2024.115062>

[27] Jappor, H.R., Khudair, S.A.M. (2017). Al-doped graphene as a sensor for harmful gases (CO, CO₂, NH₃, NO, NO₂ and SO₂). *Sensor Letters*, 15(12): 1023-1030. <https://doi.org/10.1166/sl.2017.39011023>

[28] Guo, L.Y., Xia, S.Y., Sun, H., Li, C.H., et al. (2022). A DFT study of the Ag-doped h-BN monolayer for harmful gases (NO₂, SO₂F₂, and NO). *Surfaces and Interfaces*, 32: 102113. <https://doi.org/10.1016/j.surfin.2022.102113>

[29] Malik, P., Kumari, G., Neelankshi, Sharma, P., Singh, S. (2020). Regulating electronic properties of graphene sheet via n-type doping for solar cells applications. *Journal of Materials Science: Materials in Electronics*, 31(17): 14306-14313. <https://doi.org/10.1007/s10854-020-03930-0>

[30] Ghotia, S., Rimza, T., Singh, S., Dwivedi, N., Srivastava, A.K., Kumar, P. (2024). Hetero-atom doped graphene for marvellous hydrogen storage: Unveiling recent advances and future pathways. *Journal of Materials Chemistry A*, 12(21): 12325-12357. <https://doi.org/10.1039/D4TA00717D>

[31] Wang, W., Wang, Y., Zhou, J., Luo, J., Wang, M. (2024). Modulation on electronic doping of graphene nanoribbons using alkali and oxygen atoms adsorption. *Optical and Quantum Electronics*, 56(3): 437. <https://doi.org/10.1007/s11082-023-05937-9>

[32] Yu, G., Xie, Y., Ge, Q., Dai, Q., Xu, J., Cao, H. (2022). Mechanism of ozone adsorption and activation on B-, N-, P-, and Si-doped graphene: A DFT study. *Chemical Engineering Journal*, 430: 133114. <https://doi.org/10.1016/j.cej.2021.133114>

[33] Liang, X.Y., Ding, N., Ng, S.P., Wu, C.M.L. (2017). Adsorption of gas molecules on Ga-doped graphene and effect of applied electric field: A DFT study. *Applied Surface Science*, 411: 11-17. <https://doi.org/10.1016/J.APSUSC.2017.03.178>

[34] Wang, C.B., Lu, Q., Zhang, L.L., Xu, T.T., Gong, W.J. (2022). Li-decorated borophene-graphene heterostructure under gas adsorption. *Journal of Physics and Chemistry of Solids*, 171: 111033. <https://doi.org/10.1016/j.jpcs.2022.111033>

[35] Siddique, S.A., Sajid, H., Gilani, M.A., Ahmed, E., Arshad, M., Mahmood, T. (2022). Sensing of SO_3 , SO_2 , H_2S , NO_2 and N_2O toxic gases through AZA-macrocycle via DFT calculations. *Computational and Theoretical Chemistry*, 1209: 113606. <https://doi.org/10.1016/j.comptc.2022.113606>

[36] Li, K., Li, N., Yan, N., Wang, T., Zhang, Y., Song, Q., Li, H. (2020). Adsorption of small hydrocarbons on pristine, N-doped and vacancy graphene by DFT study. *Applied Surface Science*, 515: 146028. <https://doi.org/10.1016/j.apsusc.2020.146028>

[37] Xie, T., Wang, P., Tian, C., Zhao, G., Jia, J., Zhao, C., Wu, H. (2021). The adsorption behavior of gas molecules on Co/N Co-doped graphene. *Molecules*, 26(24): 7700. <https://doi.org/10.3390/molecules26247700>

[38] Ni, J., Quintana, M., Song, S. (2020). Adsorption of small gas molecules on transition metal (Fe, Ni and Co, Cu) doped graphene: A systematic DFT study. *Physica E: Low-dimensional Systems and Nanostructures*, 116: 113768. <https://doi.org/10.1016/j.physe.2019.113768>

[39] Yin, M., Qiao, X., Wang, L., Miura, H., Suzuki, K. (2024). Strain-modulated adsorption of gas molecule on graphene: First-principles calculations. *Diamond and Related Materials*, 142: 110822. <https://doi.org/10.1016/j.diamond.2024.110822>

[40] Khudair, S.A.M., Rahman, J.H. (2020). Adsorption of gas molecules on graphene doped with mono and dual boron as highly sensitive sensors and catalysts. *Molecules*, 27(7): 2315. <https://doi.org/10.3390/molecules27072315>

[41] Xie, T., Wang, P., Tian, C., Zhao, G., et al. (2022). Adsorption characteristics of gas molecules adsorbed on graphene doped with Mn: A first principle study. *Molecules*, 27(7): 2315. <https://doi.org/10.3390/molecules27072315>

[42] Gui, Y., Peng, X., Liu, K., Ding, Z. (2020). Adsorption of C_2H_2 , CH_4 and CO on Mn-doped graphene: Atomic, electronic, and gas-sensing properties. *Physica E: Low-dimensional Systems and Nanostructures*, 119: 113959. <https://doi.org/10.1016/j.physe.2020.113959>

[43] Khudair, S.A.M., Mohaimeed, A.A. (2020). Gas sensor investigations through adsorption of toxic gas molecules on single and double vacancy graphene. *NeuroQuantology*, 18(9): 87-95. <https://doi.org/10.14704/nq.2020.18.9.NQ20221>

[44] Olatomiwa, A.L., Adam, T., Edet, C.O., Adewale, A.A., et al. (2023). Recent advances in density functional theory approach for optoelectronics properties of graphene. *Helijon*, 9(3): e14279. <https://doi.org/10.1016/j.helijon.2023.e14279>

[45] Zheng, Y., Mao, S., Zhu, J., Fu, L., Moghadam, M. (2022). A scientometric study on application of electrochemical sensors for detection of pesticide using graphene-based electrode modifiers. *Chemosphere*, 307: 136069. <https://doi.org/10.1016/j.chemosphere.2022.136069>

[46] Kuganathan, N., Anurakavan, S., Abiman, P., Iyngaran, P., Gkanas, E.I., Chromeos, A. (2021). Adsorption of lead on the surfaces of pristine and B, Si and N-doped graphene. *Physica B: Condensed Matter*, 600: 412639. <https://doi.org/10.1016/j.physb.2020.412639>

[47] Hatam, R.S., Muslim, S.I., Kadhim, R.A., Kadhim, M.M., Abbas, Z.M. (2020). Optical properties of different organic compounds: Experimental and theoretical studies. *International Journal of Pharmaceutical Research*, 12(4). <https://doi.org/10.31838/ijpr/2020.12.04.138>

[48] Gorai, P. (2025). Beginner's guide to interpreting defect and defect level diagrams. *PRX Energy*, 4(3): 032001. <https://doi.org/10.1103/jtyg-xry3>

[49] Tayyab, M., Hussain, A., Adil, W., Nabi, S., ul Ain Asif, Q. (2020). Band-gap engineering of graphene by Al doping and adsorption of Be and Br on impurity: A computational study. *Computational Condensed Matter*, 23: e00463. <https://doi.org/10.1016/j.cocom.2020.e00463>

[50] Otsuki, Y., Sugimoto, T., Ishiyama, T., Morita, A., Watanabe, K., Matsumoto, Y. (2017). Unveiling subsurface hydrogen-bond structure of hexagonal water ice. *Physical Review B*, 96(11): 115405. <https://doi.org/10.1103/PhysRevB.96.115405>

[51] Xiao, C., Li, D. (2016). Semiclassical magnetotransport in strongly spin-orbit coupled Rashba two-dimensional electron systems. *Journal of Physics: Condensed Matter*, 28(23): 235801. <https://doi.org/10.1088/0953-8984/28/23/235801>

[52] Engelhardt, F., Maaß, C., Andrada, D.M., Herbst-Irmer, R., Stalke, D. (2018). Benchmarking lithium amide versus amine bonding by charge density and energy decomposition analysis arguments. *Chemical Science*, 9(12): 3111-3121. <https://doi.org/10.1039/C7SC05368A>

[53] Sahithi, A., Sumithra, K. (2020). Adsorption and sensing of CO and NH_3 on chemically modified graphene surfaces. *RSC advances*, 10(69): 42318-42326. <https://doi.org/10.1039/D0RA06760A>

[54] Feng, J.W., Liu, Y.J., Wang, H.X., Zhao, J.X., Cai, Q.H., Wang, X.Z. (2014). Gas adsorption on silicene: A theoretical study. *Computational Materials Science*, 87: 218-226. <https://doi.org/10.1016/j.commatsci.2014.02.025>

[55] Zhang, L., Zhang, Q., Jiang, P., Liu, Y., Zhao, C., Dong, Y. (2024). Effects of alloying element on hydrogen adsorption and diffusion on α -Fe (110) surfaces: First

principles study. *Metals*, 14(5): 487. <https://doi.org/10.3390/met14050487>

[56] del Castillo, R.M., Calles, A.G., Espejel-Morales, R., Hernandez-Coronado, H. (2018). Adsorption of CO₂ on graphene surface modified with defects. *Computational Condensed Matter*, 16: e00315. <https://doi.org/10.1016/j.cocom.2018.e00315>

[57] Hassan, M., Ibrahim, I., Majid, A., Buzdar, S.A., Shaheen, H., Alarfaji, S.S., Khan, M.I. (2024). Adsorption performance of harmful gas molecules over copper decorated aluminene: A DFT study. *Adsorption*, 30(6): 1437-1451. <https://doi.org/10.1007/s10450-024-00508-0>

[58] Luo, H., Xu, K., Gong, Z., Li, N., Zhang, K., Wu, W. (2021). NH₃, PH₃, AsH₃ adsorption and sensing on rare earth metal doped graphene: DFT insights. *Applied Surface Science*, 566: 150390. <https://doi.org/10.1016/j.apsusc.2021.150390>

[59] Zhou, S., Liu, J., Pang, S., Gui, Y. (2023). Adsorption characteristics of H₂S and SO₂ gases on Cu₂O cluster-modified graphene monolayer for gas-sensing applications. *ACS Omega*, 8(48): 45763-45773. <https://doi.org/10.1021/acsomega.3c06310>

[60] Shao, L., Chen, G., Ye, H., Wu, Y., Qiao, Z., Zhu, Y., Niu, H. (2013). Sulfur dioxide adsorbed on graphene and heteroatom-doped graphene: A first-principles study. *The European Physical Journal B*, 86(2): 54. <https://doi.org/10.1140/epjb/e2012-30853-y>

[61] Xia, W., Hu, W., Li, Z., Yang, J. (2014). A first-principles study of gas adsorption on germanene. *Physical Chemistry Chemical Physics*, 16(41): 22495-22498. <https://doi.org/10.1039/C4CP03292F>